American Mineralogist, Volume 83, pages 1482–1493, 1998

Formation of lithified micritic laminae in modern marine stromatolites (Bahamas): The role of sulfur cycling

PIETER T. VISSCHER,[1,*] R. PAMELA REID,[2] BRAD M. BEBOUT,[3] SHELLEY E. HOEFT,[1] IAN G. MACINTYRE,[4] AND JOHN A. THOMPSON JR.[5]

[1]Department of Marine Sciences, University of Connecticut, Groton, Connecticut 06340, U.S.A.
[2]Division of Marine Geology and Geophysics, RSMAS, University of Miami, Miami, Florida 33149, U.S.A.
[3]NASA Ames Research Center, Moffett Field, California 94035, U.S.A.
[4]Department of Paleobiology, National Museum of Natural History, Smithsonian Institution, Washington, D.C. 20560, U.S.A.
[5]Tabor Academy, Marion, Massachusetts 02738, U.S.A.

ABSTRACT

Microbial mats on the surfaces of modern, marine stromatolites at Highborne Cay, Bahamas, were investigated to assess the role of microbial processes in stromatolite formation. The Highborne Cay stromatolitic mats contain *Schizothix* as the dominant cyanobacterium and show millimeter-scale lamination: Some layers in the mat are soft (unlithified), whereas other layers are crusty (lithified). Lithified layers within the mats correspond to micritic horizons composed of thin (20–50 μm) micritic crusts, which commonly overlie truncated, micritized carbonate sand grains. These features are identical to lithified laminae in the underlying stromatolite; the micritic crusts are similar in thickness to micritic laminae in many ancient stromatolites. Biogeochemical parameters in a representative stromatolitic mat from Highborne Cay were measured to identify the role of bacteria in precipitation and dissolution of $CaCO_3$. Depth distributions of O_2, HS^-, and pH were determined with microelectrode measurements in the field. Oxygen profiles were used to calculate photosynthesis and aerobic respiration. Sulfate reduction was determined using $^{35}SO_4^{2-}$ and sulfide oxidation potential was measured in homogenized samples. Our results indicate that cyanobacterial photosynthesis, sulfate reduction, and anaerobic sulfide oxidation in stromatolitic mats at Highborne Cay are responsible for $CaCO_3$ precipitation, whereas aerobic respiration and aerobic sulfide oxidation cause $CaCO_3$ dissolution. A close coupling of photosynthesis and aerobic respiration in the uppermost few millimeters of the mats results in no, or very little, net lithification. Sulfur cycling, on the other hand, shows a close correlation with the formation of lithified micritic layers. Photosynthesis, combined with sulfate reduction and sulfide oxidation results in net lithification. Sulfate reduction rates are high in the uppermost lithified layer and, on a diel basis, consume 33–38% of the CO_2 fixed by the cyanobacteria. In addition, this lithified layer contains a significant population of sulfide-oxidizing bacteria and shows a high sulfide oxidation potential. These findings argue that photosynthesis coupled to sulfate reduction and sulfide oxidation is more important than photosynthesis coupled to aerobic respiration in the formation of lithified micritic laminae in Highborne Cay stromatolites.

INTRODUCTION

Stromatolites record the interactions of biological and geological processes throughout the 3.5 billion year history of life on Earth (Awramik 1992). Earth's oldest macrofossils, stromatolites are not individual organisms, but rather lithified, laminated sedimentary structures produced by the activities of benthic microbial mats. Interpretation of ancient stromatolites, which dominate the fossil record for 85% of Earth's history, is limited by a lack of understanding of geomicrobiological processes in modern stromatolites. Until recently, modern stromatolites forming in open marine settings, environments in which many ancient stromatolites are thought to have formed, were unknown.

Modern stromatolites forming in open ocean water of normal marine salinity were first discovered in the Schooner Cays, on the east margin of Exuma Sound, Bahamas (Fig. 1), in the early 1980s (Dravis 1983). Since then, they have been found at numerous locations throughout the Exuma Cays, on the west margin of Exuma Sound (Fig. 1; Dill et al. 1986; Reid and Browne 1991; Reid et al. 1995). Typically forming domal buildups ranging in height from several centimeters to over 2 m, these Exuma stromatolites are well-laminated structures composed

* E-mail: visscher@uconnvm.uconn.edu

0003–004X/98/1112–1482$05.00

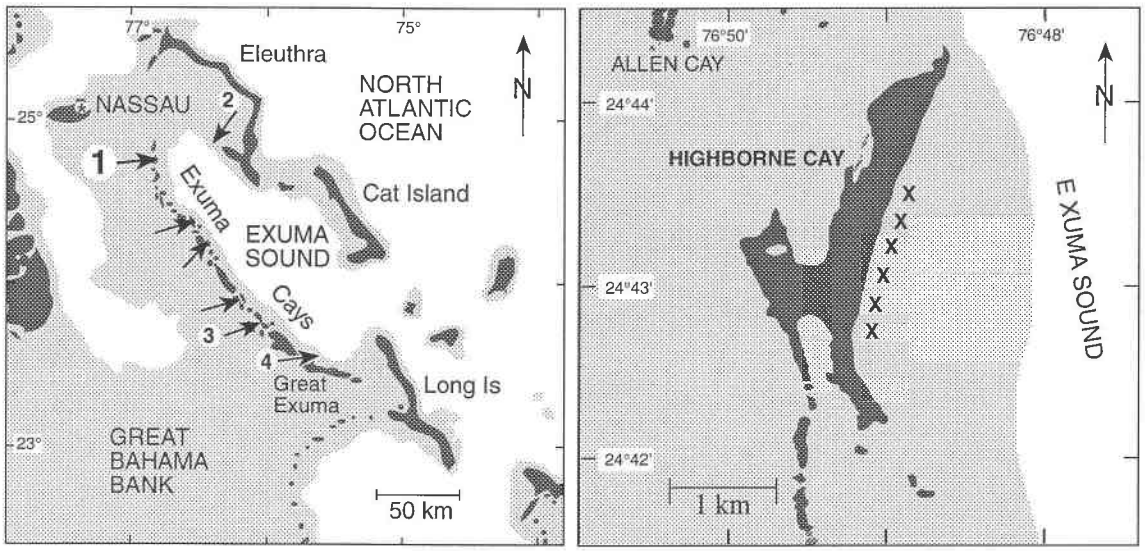

FIGURE 1. (**Left**) Index map showing stromatolite locations (arrows) on the margins of Exuma Sound: 1. Highborne Cay, study site for this paper; 2. Schooner Cays (Dravis 1983); 3. Lee Stocking Island (Dill et al. 1986); 4. Stocking Island (Reid and Browne 1991; Macintyre et al. 1996; Steneck et al. 1997); unnumbered sites (Reid et al. 1995). (**Right**) Map of Highborne Cay, showing the location of the stromatolites (xxxx) in a fringing reef along the eastern margin.

mainly of fine-grained carbonate sand (125–250 μm). Well-laminated stromatolites show gradational transitions to unlaminated thrombolites (Feldmann 1995; Reid et al. 1995; Golubic and Browne 1996; Macintyre et al. 1996).

Lamination in Exuma stromatolites reflects periodic episodes of lithification. As readily observed in sawed slabs, cemented layers 0.5 to 3 mm thick stand out in relief on cut surfaces (Fig. 2a). In thin section, these lithified layers are subtle, but distinct, corresponding to micritic horizons with three characteristic features (Fig. 2b): (1) a thin (20–40 μm thick) crust of microcrystalline carbonate (micrite) occurs at the top of most lithified layers; (2) the upper surfaces of sand grains immediately below these crusts are commonly intensely microbored and truncated; and (3) sand grains in the lithified layer are altered to structureless, micritic textures (i.e., they are

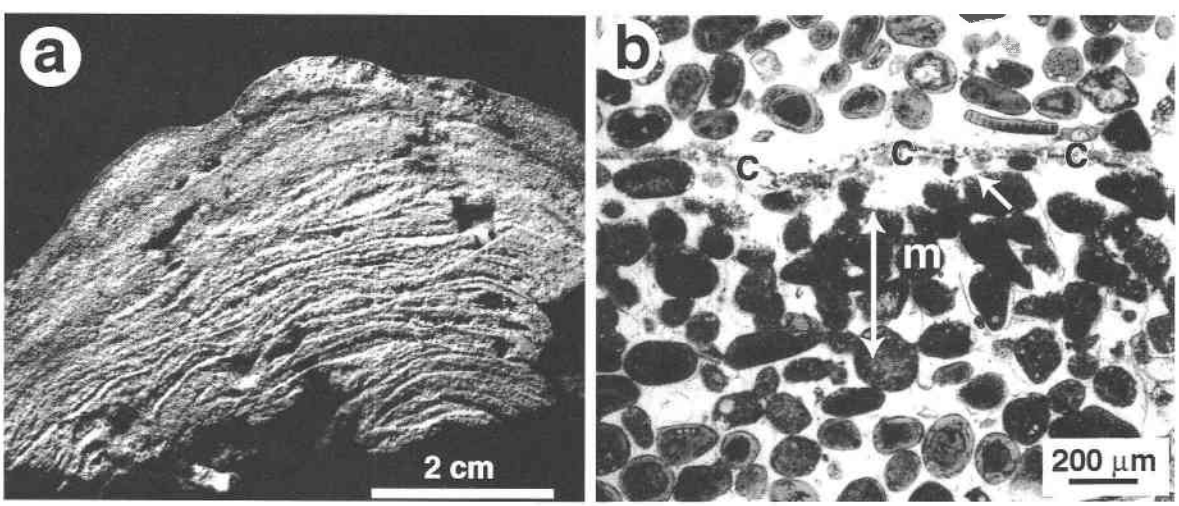

FIGURE 2. (**a**) Sawed section through a small stromatolite head. Note the millimeter-scale lamination, which reflects differential lithification; cemented layers stand out in relief on the cut surface. Sample 6/97.NS.8p, Highborne Cay, Bahamas. (**b**) Thin section photomicrograph showing a typical lithified layer within an Exuma stromatolite. Note the micritic crust (c), which overlies micritized sand grains (m) that appear to be welding together. The double-headed arrow indicates the horizon of micritized grains; compare these structureless grains with the grains showing translucent ooid coatings in the unlithified layers at the top and bottom of the photo. Some of the micritized grains are truncated below the micritic crust (right arrow). Sample 1/97.NS.3, Highborne Cay, Bahamas.

micritized) and are joined at point contacts by micrite cement (see also Reid and Browne 1991; Reid et al. 1995; Golubic and Browne 1996; Macintyre et al. 1996). Macintyre et al. (1996) suggested that the truncation of grains along the tops of these lithified horizons is a result of bioerosion by microboring, but argued that micritization of grains below the truncated surfaces results from grain recrystallization, rather than by the infilling of microborings (Macintyre et al. 1996). Further discussion concerning the role of microboring in inducing recrystallization in these micritized grains is in preparation.

Some previous studies have focused on textural differences between Exuma and ancient stromatolites, suggesting that the modern forms, which are sandy, are inappropriate analogs for ancient stromatolites, which are typically micritic (e.g., Awramik and Riding 1988; Riding et al. 1991; Riding 1994). These studies, however, overlooked a fundamental similarity between the modern and ancient structures: Lamination in both reflects periodic formation of lithified micritic horizons. Moreover, the micritic crusts in Exuma stromatolites are remarkably similar in thickness to micritic laminae in many ancient stromatolites (e.g., Walter 1983; Bertrand Sarfati 1976; Monty and Mas 1981).

Exuma stromatolites thus offer a unique opportunity to investigate the formation of lithified micritic laminae in stromatolites forming in a modern marine environment. Initial observations indicating that lithified micritic laminae in Exuma stromatolites form within microbial mats at the surface of these structures led to the present study, which examines microbial processes involved in this lithification process.

Microbial processes are well known to cause precipitation and dissolution of $CaCO_3$. Photosynthesis of cyanobacteria has, for example, long been linked to $CaCO_3$ precipitation (e.g., Dalrymple 1965).

$$\begin{aligned} CO_2 + H_2O &\rightarrow [CH_2O] + O_2 \\ HCO_3^- &\rightarrow CO_2 + OH^- \\ Ca^{2+} + HCO_3^- &\rightarrow CaCO_3 + H^+ \\ H^+ + OH^- &\rightarrow H_2O \\ \hline 2HCO_3^- + Ca^{2+} &\rightarrow [CH_2O] + CaCO_3 + O_3 \end{aligned} \quad (1)$$

(net: $+1\ CaCO_3$)

Photosynthetic CO_2 fixation produces organic carbon (CH_2O), which may, in turn, be oxidized via aerobic respiration

$$\begin{aligned} [CH_2O] + O_2 &\rightarrow HCO_3 + H^+ \\ CaCO_3 + H^+ &\rightarrow HCO_3^- + Ca^{2+} \\ \hline [CH_2O] + CaCO_3 + O_2 &\rightarrow 2HCO_3^- + Ca^{2+} \end{aligned} \quad (2)$$

(net: $-1\ CaCO_3$)

Aerobic respiration by heterotrophic bacteria results in $CaCO_3$ dissolution (e.g., Jørgensen and Cohen 1977; Krumbein et al. 1977; Gerdes et al. 1985). Organic carbon produced by photosynthesis also may be oxidized anaerobically by sulfate reduction. Reduction of sulfate yields HCO_3^- and HS^- and results in $CaCO_3$ precipitation (3) (Chafetz and Buczynski 1992).

$$\begin{aligned} 2[CH_2O] + SO_4^{2-} + OH^- &\rightarrow 2HCO_3^- + HS^- + H_2O \\ HCO_3^- + Ca^{2+} &\rightarrow CaCO_3 + H^+ \\ HCO_3^- + H^+ &\rightarrow CO_2 + H_2O \\ \hline 2[CH_2O] + SO_4^{2-} + OH^- + Ca^{2+} &\rightarrow \begin{cases} CaCO_3 + CO_2 + 2H_2O \\ + HS^- \end{cases} \end{aligned} \quad (3)$$

(net: $+1\ CaCO_3$)

The sulfide is oxidized in chemolithotrophic respiration, either with O_2 (aerobic) or with NO_3^- (anaerobic) (Friedman et al. 1973, Walter et al. 1993).

$$\begin{aligned} HS^- + 2O_2 &\rightarrow SO_4^{2-} + H^+ \\ CaCO_3 + H^+ &\rightarrow HCO_3^- + Ca^{2+} \\ \hline HS^- + 2O_2 + CaCO_3 &\rightarrow SO_4^{2-} + Ca^{2+} + HCO_3^- \end{aligned} \quad (4a)$$

(net: $-1\ CaCO_3$)

$$\begin{aligned} 5HS^- + 8NO_3^- &\rightarrow 5SO_4^{2-} + 4N_2 + H_2O + 3OH^- \\ 3HCO_3^- + 3Ca^{2+} &\rightarrow 3CaCO_3 + 3H^+ \\ 3OH^- + 3H^+ &\rightarrow 3H_2O \\ \hline 5HS^- + 8NO_3^- + 3HCO_3^- + 3Ca^{2+} &\rightarrow \begin{cases} 3CaCO_3 + 4N_2 + 4H_2O \\ + 5SO_4^{2-} \end{cases} \end{aligned} \quad (4b)$$

$$\left(\text{net: } +\frac{3}{5}\ CaCO_3\right)$$

In several microbial mat studies in stagnant, often hypersaline lagoons, a correlation was found between the presence of acid volatile sulfides (produced by sulfate-reducing bacteria) and potential of $CaCO_3$ precipitation (Krumbein 1979; Krumbein et al. 1979; Lyons et al. 1984). Similarly, involvement of anaerobic bacteria, presumably that of sulfate reducers, was hypothesized in dolomite formation (Vasconcelos et al. 1995; Vasconcelos and McKenzie 1997). Although not supported by measurements, Walter et al. (1993) suggested the importance of HS^- oxidation in dissolution and recrystallization of $CaCO_3$ in carbonate platform sediments.

To examine the role of different functional groups of bacteria [i.e., oxygenic phototrophic bacteria (Eq. 1), aerobic heterotrophic microbes (Eq. 2), sulfate-reducing bacteria (Eq. 3), and sulfide-oxidizing bacteria (Eq. 4)] in the formation of lithified micritic horizons in Exuma stromatolites, we measured biogeochemical gradients, which are the result of the diffusion of metabolic products. In addition, we determined the activities of the metabolic reactions, summarized above, in these mats. Our goal was to assess the relative importance of photosynthesis, aer-

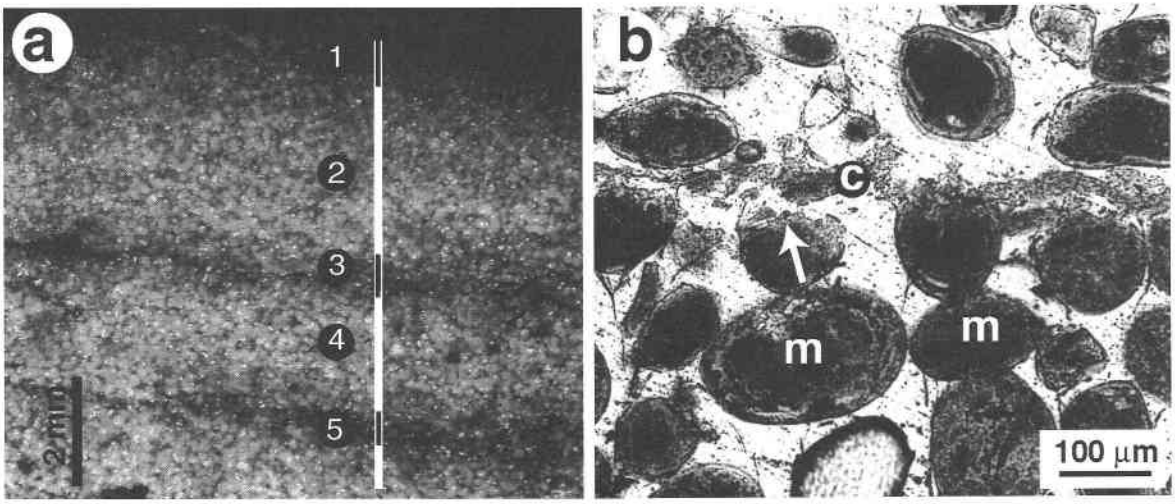

FIGURE 3. (a) Binocular photomicrograph showing the microbial mat analyzed for the present study. Five distinct layers are visible: Layer 1, which is unlithified, is caramel colored; Layers 3 and 5, which are crusty, are gray-green; and Layers 2 and 4, also unlithified, are white. Sample 6/97.NS.8n, Highborne Cay, Bahamas. (b) Thin section photomicrograph showing the upper part of Layer 3 of the study mat. Note the micritic crust (c), which occurs at the top of Layer 3; the truncated grains below this crust (arrow), and the micritized grains (m), which have lost, or are losing, evidence of their original ooid coatings. Sample 6/97.NS.8n, Highborne Cay, Bahamas.

obic respiration, sulfate reduction, and sulfide oxidation in stromatolite formation.

SITE SELECTION AND SAMPLE DESCRIPTION

Our study was conducted at Highborne Cay, Bahamas (Fig. 1). Located at the north end of the Exuma Cays, Highborne Cay is bordered on the west by Great Bahama Bank, where water depths are less than 10 m. On the east, Highborne Cay is fringed by a shelf, 1–2 km wide and up to 40 m deep; the shelf edge marks a drop off into Exuma Sound, where depths exceed 2000 m. Stromatolites occur in a fringing reef complex along the east side of the island, which is exposed to the open water conditions of Exuma Sound. The reef complex at Highborne Cay is similar to that previously described at Stocking Island (Macintyre et al. 1996; Steneck et al. 1997): Stromatolites are found in the back reef area of a coralline algal ridge, where they form intertidal and shallow subtidal buildups up to 0.5 m thick. Highborne Cay was chosen as the study site because stromatolites at this locality exhibit exceptionally well-developed lamination.

For our investigation of microbial processes forming Highborne Cay stromatolites, we analyzed microbial mats at the surfaces of these structures. In this paper, we report a detailed study of one such mat; this mat appears to be a representative sample of stromatolite-forming mats in the Exuma region.

The microbial mat that is the focus of our paper forms the uppermost few centimeters of a subtidal stromatolite that was growing in about 20 cm of sea water at mean-low tide. This mat shows five distinct layers (Fig. 3a). Layer 1, at 0–0.5 mm, is caramel colored and soft (unlithified); Layers 2 and 4 are white and soft; and Layers 3 and 5 are green-gray and crusty (lithified). Optical microscopy shows that the mat is a prokaryotic community dominated by the cyanobacteria *Schizothrix* sp.; *Schizothrix* filaments are abundant in Layers 1, common in Layers 3 and 5 and scarce in Layers 2 and 4. In addition to *Schizothrix,* endolithic cyanobacteria are also abundant in Layer 3. A petrographic thin section of this mat shows that Layers 3 and 5 are micritic horizons with the characteristic features of lithified layers in Exuma stromatolites: Thin micrite crusts overlie truncated, micritized grains (Fig. 3b).

MATERIALS AND METHODS

Microelectrode measurements

Microelectrodes were used to make field measurements of O_2, HS^-, and pH gradients in the upper 2 cm of the stromatolite from 6:00 a.m. until 2:00 a.m. the following morning. Depth profiles of oxygen and sulfide were determined using needle electrodes with an outer diameter of 0.8 mm (Visscher et al. 1991); pH was measured with an electrode encased in a 1 mm hypodermic needle (Diamond General, Ann Arbor, Michigan). During profiling, the stromatolite sample (80 × 50 mm, approximately 30–40 mm thick, embedded in 50 mm of sand from the site) was removed from its growth site in 30–70 cm water depth in the reef lagoon and electrode measurements were carried out in 2–4 cm of stagnant water; between measurements, the stromatolite sample was returned to its original site. Three profiles were measured and averaged during each sampling to account for heterogeneity of the stromatolite mat. Typically, the maximum depth of O_2 penetration was within 0.4 mm between replicates; depth

of first appearance of HS^- as within 0.8 mm between replicate measurements. Ambient light was recorded with a LiCor LI-1000 light meter equipped with a quantum sensor (LiCor, Lincoln, Nebraska).

Oxygen profiles were used to calculate aerobic respiration and photosynthesis. For aerobic respiration, O_2 profiles were measured in the light, then sample and electrode were covered and O_2 profiling was repeated after 1 and 5 min of darkness. Aerobic respiration was calculated from the initial slope of O_2 consumption and was normalized for O_2 concentrations within each layer. Photosynthesis was determined as the increase of the O_2 concentration with depth upon exposure to light (Revsbech and Jørgensen 1985), assuming steady state was reached after 5 min. Similar results were obtained using O_2 profiles measured using glass microelectrodes with 20 μm tip diameter (Diamond General, Ann Arbor, Michigan) and needle microelectrodes (Microscale Measurements, The Netherlands).

Rate measurements of microbial activities

Upon completion of field measurements for a 24 h cycle, the stromatolite was brought to the laboratory and sectioned within 30 min. One half was used for photography and thin sectioning, whereas the microbial mat on the surface of the other half was dissected into the five layers shown in Figure 3a. Subsamples from individual layers were incubated to determine sulfate reduction rates and to determine the population size of sulfate-reducing bacteria and aerobic sulfide oxidizing bacteria. Sulfate reduction was determined with $^{35}SO_4^{2-}$ (Fossing and Jørgensen 1989) in serum bottles (37 mL) that were either flushed with N_2 or that contained air as the headspace gas; three replicate incubations were done for each layer. Microbial populations of sulfate-reducing bacteria and sulfide-oxidizing bacteria were determined with most-probable number (MPN) incubations in specific synthetic nutrient medium after serial dilution in autoclaved sea water (Hines et al. 1996; Visscher and Van Gemerden 1993). Final scores were taken after six weeks and populations calculated according to De Man (1975).

Measurements of potential microbial activity

Laboratory analyses of stromatolitic mats also included slurry experiments to investigate respiration potential. For these experiments, material from Layers 1–3 (i.e., the uppermost 5 mm of the mat) was homogenized by stirring in sterilized sea water (1:1 vol. mat/vol. sea water) collected from the field site. Potential rates of aerobic respiration and sulfate reduction (anaerobic respiration) were determined by supplementing the homogenized slurries of stromatolite mat with organic carbon. Effects of substrate additions were assessed by comparison with endogenous rates (no substrate addition). Respiration rates were determined by the decline in $[O_2]$ and increase in $[HS^-]$ during aerobic respiration and sulfate reduction, respectively. Respiration rates were measured in a closed 20 mL chamber with an oxygen microelectrode or sulfide needle electrode. For aerobic respiration, the homogenate was aerated; for sulfate reduction, the slurry was purged with N_2 for 15 min. All experiments were replicated. Triplicate organic carbon additions included: acetate, lactate, ethanol (each at 10–50 μ*M* final concentration), and *Schitzothrix* exopolymer (EPS; 1.67, μg/mL). Sulfate reduction potential upon thiosulfate addition (100 μ*M*) was also determined. Similar to sulfate, thiosulfate can be reduced to HS^-, which adds to $CaCO_3$ precipitation (compare with Eq. 3).

Slurry experiments of mat homogenates from the upper 5 mm were also used to assess the respiration potential of sulfide oxidation (chemolithotrophic respiration). For this, either sulfide or thiosulfate were added in the presence of O_2 (aerobic chemolithotrophic respiration) and under anoxic conditions, supplemented with nitrate (denitrifying, or anaerobic chemolithotrophic respiration). The same experimental conditions as for organic carbon additions were employed; HS^- and $S_2O_3^{2-}$ were added to a final concentration of 10–50 μ*M* and nitrate to a final concentration of 500 μ*M*. Autoclaved slurries were used to account for abiotic (chemical) loss.

Results

Biogeochemical gradients

Concentration profiles of O_2 and HS^- in the stromatolite mat showed distinct diel fluctuations (Fig. 4). This diel pattern of O_2 fluctuation is typical for microbial mats (Visscher and Van den Ende 1994). Oxygen penetration was limited to 2 mm at sunrise and showed no subsurface maximum. During the day, O_2 penetration increased to 4–5 mm, due to increased photosynthetic activity. Values of more than twice O_2 saturation were measured during the early afternoon at 1.7 mm depth. Toward the end of the afternoon, the oxycline was at 3 mm (top of Layer 3), despite significant light availability (210 μE/m²/s). O_2 was only detected in the upper 0.75–1 mm of the stromatolitic mat throughout the night.

Sulfide appeared within millimeters of the surface in the stromatolite mat: HS^- was detected at 2.5 mm at sunrise, 7 mm at 1:00 p.m., 3.5 mm at 6:00 p.m., and 1 mm at 2:00 am. The concentration of HS^- peaked at 125–260 μ*M* at 12–16 mm during daytime and 300 μ*M* at 8 mm during the night. During most of the daylight hours, the O_2/HS^- interface was well defined and found at a depth of 3–5 mm, within Layer 3, which is a lithified horizon. During the early afternoon, O_2 and HS^- profiles were separated by 1–2 mm, possibly due to high rates of aerobic and anaerobic respiration (see below).

Gradients of pH within the stromatolite mat (Fig. 4) showed less diel variability than the O_2 and HS^- profiles. From late afternoon until early morning, pH values gradually increased with depth. Surface values of pH ~7.5 were slightly lower than ambient sea water, with a pH of 7.9; mat pH progressively increased to values of about 8–8.2 at 5 mm depth. The lower pH values at the surface of the stromatolite may be associated with production of

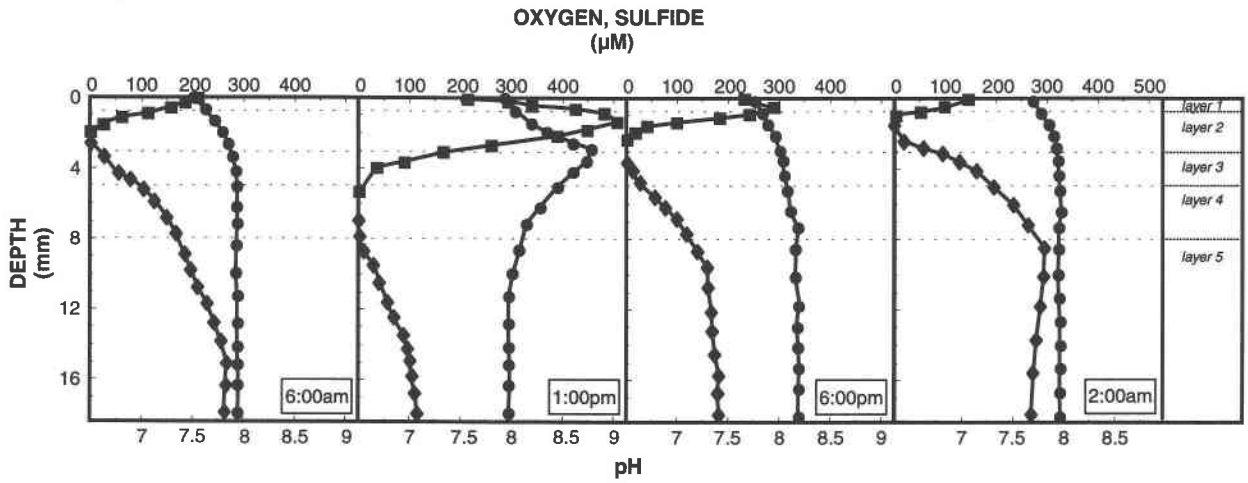

FIGURE 4. Depth distribution of O_2 (filled box), HS^- (filled diamond) and pH (filled circle) in the upper 16 mm of the stromatolite mat measured in situ with microelectrodes. Measurements were taken on June 14–15, 1997. Ambient light intensity and was 30 μE/m²/s (6:00 a.m.), 1760 μE/m²/s (1:00 p.m.), 210 μE/m²/s (6:00 p.m.), and 0 μE/m²/s (2:00 a.m.); the pH of ambient seawater is 7.9.

organic acids through excretion by phototrophs during photorespiration and formation of H_2SO_4 from HS^- oxidation (Eq. 3). A major departure from this trend of gradual increase of pH with depth was observed in early afternoon. At this time, a peak in pH of 8.7 occurred just below the depth of maximum O_2 concentration and coinciding with the top of lithified Layer 3. During this early afternoon period, pH values at depths of 1 mm to 8 mm were higher than the pH of ambient sea water. High rates of photosynthetic CO_2 fixation and perhaps sulfate reduction (i.e., removal of H_2SO_4) could have contributed to this rise in pH. pH values at 3 mm, which is the top of Layer 3, ranged from 7.85 at night to 8.75 during the early afternoon.

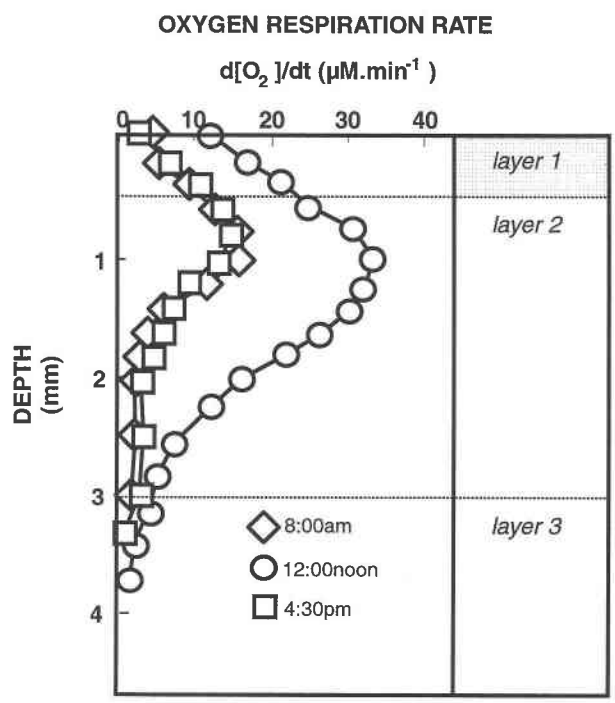

FIGURE 5. Rate of photosynthesis in the stromatolite mat determined in the field with microelectrodes using the dark-light shift technique (see text). Ambient light intensity and was 1250–1850 μE/m²/s (12:30 p.m.) and 200–220 μE/m²/s (5:30 p.m.).

Microbial rates

Photosynthesis, aerobic respiration, and sulfate reduction were active within the stromatolite mat. The net rate of photosynthesis (Fig. 5) showed a maximum primary production of 60 μ*M*/min O_2 at 12:30 p.m. at the interface of Layers 1 and 2, when the light intensity fluctuated between 1250 and 1850 μE/m²/s. This corresponded to an O_2 (hence $\{CH_2O\}$; see Eq. 1) production rate of approximately 410 nmol/cm²/h. Late in the afternoon light intensity decreased to 200–220 μE/m²/s, the photosynthetic rate also decreased to 30 μ*M*/min O_2 corresponding to O_2 (or $\{CH_2O\}$) production rates of 120 nmol/cm²/h. Light intensity peaked at 2139 μE/m²/s between 1:30–2:00 p.m..

Aerobic respiration rates (Fig. 6) showed patterns of daytime variability that were similar to those seen in the O_2 and photosynthesis profiles (Figs. 4 and 5): maximum rates of aerobic respiration occurred in early afternoon, reaching values of 33 μ*M*/min O_2 just below the interface of Layers 1 and 2; early morning and late afternoon rates were lower, peaking at 15 μ*M*/min O_2. Integrated over depth, respiration rates were 270 μ*M*/h O_2 in midday and 50 μ*M*/h O_2 during early morning and late afternoon. At night, aerobic respiration was dependent on diffusion of O_2 from the overlying water and rates were near zero (data not shown).

Measurements of sulfate reduction rates in individual layers during the day and in the night show that the high-

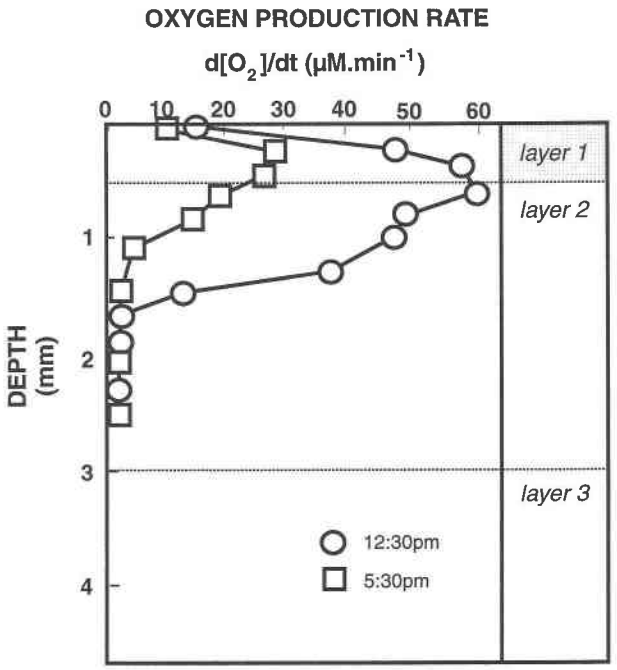

FIGURE 6. Oxygen respiration rate in the stromatolite mat. Measurements were taken in the field and rates calculated from the dark consumption in the dark (see text).

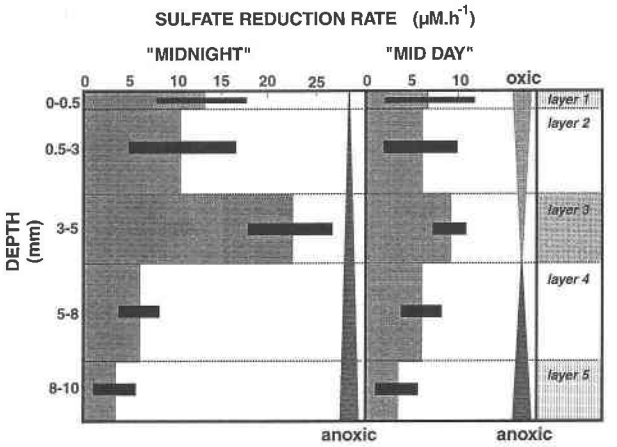

FIGURE 7. Sulfate reduction rate within individual layers of the stromatolite mat. Sub-samples were incubated with $^{35}SO_4^{2-}$ under either oxic or anoxic atmosphere (indicated by the vertical arrows in both panels). Error bars indicate the standard deviation of triplicate samples.

est rates are in Layer 3, regardless of whether O_2 was present or absent (Fig. 7). At midday, when the oxicline was located at approximately 5 mm depth near the bottom of Layer 3 (1:00 p.m. profile, Fig. 4), the sulfate reduction rate in Layer 3 was 9 μM HS^- produced (or SO_4^{2-} reduced; Eq. 3) per hour. At night, when almost the entire stromatolite mat was anoxic, the sulfate reduction rate in Layer 3 was 23 μM/h. Sulfate reduction was also active at the surface of the stromatolite, in Layer 1, although rates appeared lower than in Layer 3, ranging from 7 μM/h during the day, in the presence of O_2, to 13 μM/h at midnight, without O_2. Depth-integrated sulfate reduction rates ranged from 7.5–12 nmol/cm²/h HS^-. The rate of HS^- oxidation is difficult to measure because of formation of many different reaction products. Some of these products (e.g., $S_2O_3^{2-}$) are rapidly reduced back to HS^- by sulfate-reducing bacteria. However, based on the location of the oxycline, the rate of HS^- oxidation is expected to peak in Layer 3.

Bacterial populations

MPN incubations revealed distinct variations in the abundance of sulfate-reducing and sulfide-oxidizing bacteria in individual layers of the stromatolite mat (Fig. 8). Maximum population densities of sulfate-reducing bacteria ($8 \cdot 10^5$ cells/cm³) and sulfide-oxidizing bacteria ($2 \cdot 10^4$ cells/cm³) are found within lithified Layer 3. Indeed, sulfate-reducing bacteria were two orders of magnitude more abundant in Layer 3 than in any other layer. Anoxygenic phototrophic and denitrifying sulfide-oxidizing populations were only associated with Layers 2 and 3. Both were slightly larger in Layer 3 and were $<5 \cdot 10^2$ cells/cm³ (data not shown).

Respiration potential

Potential rates of aerobic respiration and sulfate reduction, as determined by slurry experiments, indicate severe organic carbon limitation within the mats. Addition of

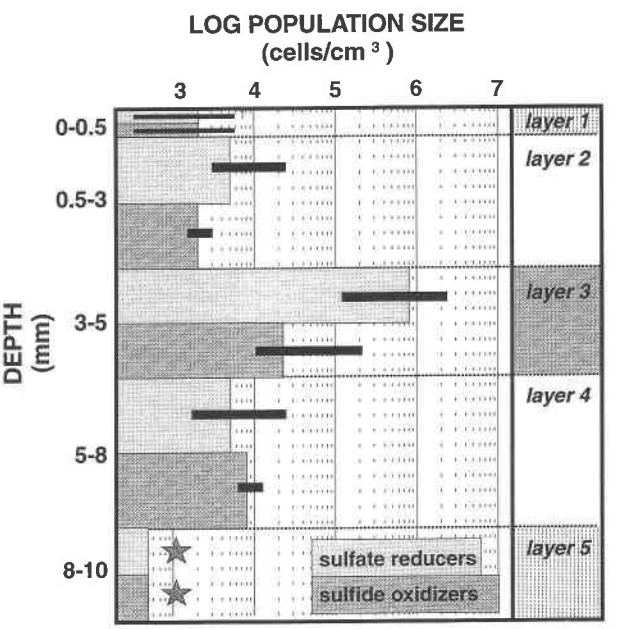

FIGURE 8. Depth distribution of microbial populations of sulfate-reducing bacteria (light bars) and sulfide-oxidizing bacteria (dark bars) in Layers 1 through 5. The error bars indicate the 95% confidence interval; open stars indicate a population size of $<5 \cdot 10^2$ cells/cm³.

TABLE 1. Rates of oxygen uptake and sulfide production by bacteria in stromatolite homogenate

Organic carbon source	Oxygen respiration rate $d[O_2]/dt$ (μmol/mL/h)	Sulfate reduction rate $d[S^{2-}]/dt$ (μmol/mL/h)
Acetate	84 (4)	115 (21)
Lactate	63 (7)	46 (7)
EPS	48 (11)*	61 (10)†
Ethanol	74 (8)	50 (3)
Endogenous rate	8 (2)	11 (2)

Notes: Oxic and anoxic conditions are shown. Organic carbon additions stimulated aerobic respiration or sulfate reduction upon which rates were determined from the initial slope of O_2 uptake or HS^- production. EPS isolated from a *Schizothrix* culture was consumed after a considerable lag phase. Numbers indicate mean of two replicate experiments, each receiving three different concentrations of organic carbon.

* After >30 min lag.

† After 5–10 min lag.

TABLE 2. Sulfide and thiosulfate oxidation rates in homogenized stromatolite samples

Electron acceptor	HS^- Oxidation rate (μmol/mL/h) $d[O_2]/dt$	HS^- Oxidation rate (μmol/mL/h) $d[HS^-]/dt$	$S_2O_3^{2-}$ Oxidation rate $d[O_2]/dt$ (μmol/mL/h)
Oxygen	41 (8)	36 (6)	109 (21)*
Nitrate	–	23 (10)	–
Endogenous rate	14 (3)†	9 (2)†	6 (2)‡

Notes: Aerobic HS^- oxidation was measured as decrease of $[O_2]$ and $[HS^-]$; $S_2O_3^{2-}$ oxidation is expressed as decline in $[O_2]$. Anaerobic oxidation of HS^- was measured under denitrifying (i.e., nitrate-respiring) conditions as the removal of sulfide from the homogenate.

organic compounds resulted in marked increases of aerobic respiration and sulfate reduction above endogenous rates (Table 1). Aerobic respiration, as determined by O_2 consumption ($d[O_2]/dt$), responded immediately to the addition of small organic substrates. Increase in respiration was the highest for acetate and ethanol, which effects did not differ significantly. When the mat homogenate was initially supplemented with *Schizothrix* exopolymer (EPS), a complex organic substrate, aerobic respiration did not increase until after a lag time of 30–40 min; successive additions of EPS were consumed without lag.

Sulfate reduction rates, measured as sulfide production ($d[HS^-]/dt$) showed similar patterns of increased activity upon addition of organic carbon. The organic carbon source that stimulated sulfate reduction the most was acetate, which enhanced sulfate reduction more than it stimulated aerobic respiration. EPS was consumed by sulfate reduction with a shorter lag than for aerobic respiration, possibly due to a rapid fermentation of this organic compound and subsequent utilization of the fermentation products (such as acetate, lactate, and ethanol) by sulfate-reducing bacteria. Sulfate reduction stimulated by thiosulfate reduction was also measured as the increase of HS^- in an anoxic homogenate. After a brief lag (5–10 min), the rate of HS^- production from 100 μ*M* $S_2O_3^{2-}$ was 82 μmol/mL/h. This demonstrates that the thiosulfate available in the mat, in addition to being oxidized to SO_4^{2-} (see below), can be reduced in part to HS^- (Jørgensen 1990; Visscher et al. 1992).

Sulfide and thiosulfate oxidation potential (Table 2), as measured in slurry experiments, indicate a high potential rate of immediate biological re-oxidation of HS^- produced by sulfate-reducing bacteria. Anaerobic sulfide oxidation, with nitrate as electron acceptor, was only slightly and not significantly lower than aerobic oxidation (23 ± 10 and 36 ± 6 μmol/mL/h HS^-, respectively), demonstrating that a significant amount of sulfide can be oxidized in the absence of O_2.

DISCUSSION

Biogeochemical gradients in stromatolitic mats at Highborne Cay (Fig. 4) indicate distinct spatial and temporal distributions of photosynthesis, aerobic respiration, and sulfur cycling (i.e., SO_4^{2-} reduction and HS^- oxidation) within individual layers (Fig. 9). Layer 1 is associated with high cyanobacterial biomass, and thus with maxima in rates of photosynthesis and aerobic respiration. Layer 3 contains a high biomass of sulfur bacteria and cyanobacteria, including endolithic species, and is associated with dynamic sulfur cycling. The microbial processes listed above are, moreover, known to induce precipitation and dissolution of $CaCO_3$ (Eqs. 1–4). Inferred interactions of these various precipitation and dissolution events in creating the observed patterns of lithification and characteristic features of the lithified micritic horizons in Exuma stromatolites are discussed below.

Photosynthesis and aerobic respiration

Photosynthesis and aerobic respiration are active in Layer 1 and in the upper part of Layer 2 of the stromatolite mat during the day (Figs. 4, 5, and 9). High rates of photosynthesis result in CO_2 depletion and corresponding $CaCO_3$ precipitation, assuming sufficient Ca^{2+} availability (Eq. 1). Reestablishment of the carbonate equilibrium ($HCO_3^- \rightarrow CO_2 + OH^-$) in response to CO_2 depletion results in an increase of pH (Visscher and van Gemerden 1991).

As the CO_2 concentration declines due to photosynthetic removal, pH values increase. Relatively low $[CO_2]$ and high $[O_2]$ occur during the afternoon. As a result, the key enzyme in CO_2 fixation, Ribulose Bisphosphate Carboxylase-Oygenase, switches from predominantly CO_2 (carboxylation) to predominantly O_2 (oxygenation) utilization. This results in photorespiration and production of C_2 compounds (e.g., glycolate), a significant fraction of which is excreted and available for aerobic and anaerobic respiring bacteria. Carbon availability stimulates sulfate reduction (Table 1; see below), and thus enhances H_2SO_4 removal causing the pH to further increase during the daytime, especially in Layer 3 (Fig. 6).

Increases in pH in Layer 2, from values of 7.6–7.7 early in the morning to values of up to 8.7 in the afternoon (Fig. 4), are probably mainly related to photosyn-

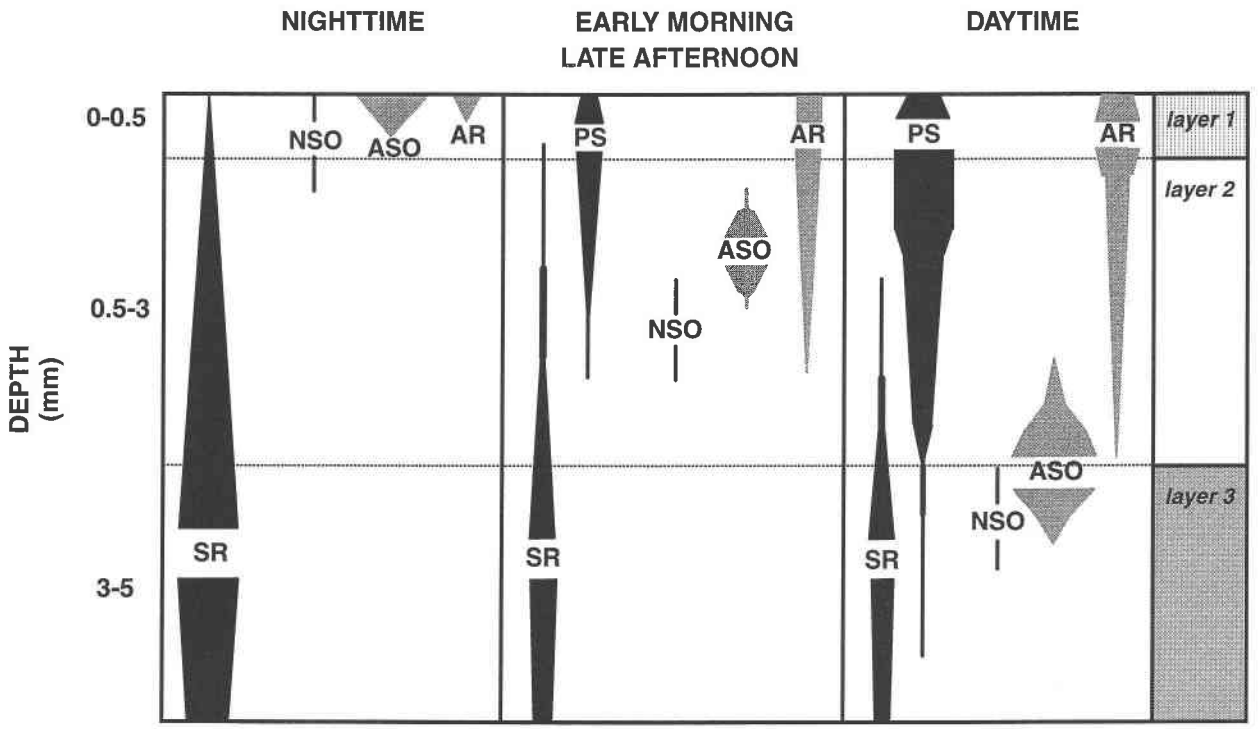

FIGURE 9. Schematic representation showing the spatial and temporal distribution of microbial processes resulting in precipitation and dissolution of carbonate (see Eqs. 1–4) in a stromatolitic mat from Highborne Cay. Left panel depicts nighttime, middle panel transient hours (1–2 h in early morning and late afternoon) and right panel daytime processes. PS = photosynthesis, AR = aerobic respiration, SR = sulfate reduction, ASO = aerobic sulfide oxidation, NSO = denitrifying sulfide oxidation (anaerobic respiration). Arrow lengths indicate depth zones over which the respective processes are active; arrow widths indicate the relative importance of the processes; light arrows are associated with $CaCO_3$ dissolution; dark arrows are indicative of $CaCO_3$ precipitation.

thetic activity, which predominates in Layer 1 (Fig. 5). In addition, sulfate reduction, which predominates in Layer 3 (Fig. 7), may also contribute to the observed pH increase. High pH favors the reaction: $HCO_3^- + OH^- \rightarrow HCO_3^{2-} + H_2O$, which leads to $CaCO_3$ precipitation.

Aerobic respiration depends on $\{CH_2O\}$ and O_2 availability (Eq. 2) and is closely associated with photosynthesis in space and time (Figs. 5 and 6). Oxidation of organic carbon during aerobic respiration yields H^+, decreasing the pH (Eq. 2). Low pH favors the reaction: $HCO_3^- + H^+ \rightarrow CO_2 + H_2O$, which results in $CaCO_3$ dissolution. Thus, photosynthesis and aerobic respiration have opposite effects on $CaCO_3$; the former leads to precipitation, while the latter dissolves $CaCO_3$. If the rates of photosynthesis and aerobic respiration were similar, no net lithification would result in Layers 1 and 2. However, as discussed below, photosynthesis is supporting both aerobic and anaerobic respiration. This could lead to some net carbonate precipitation within Layer 1 and the top of Layer 2.

Sulfur cycling: Sulfate reduction and sulfide oxidation

In contrast to photosynthesis and respiration, which are most active in unlithified Layers 1 and 2, the highest rates of sulfate reduction, during both the day and night, were found deeper in the mat, within Layer 3 (Figs. 5 and 7), a lithified horizon. Sulfate reduction mediates $CaCO_3$ precipitation through HCO_3 production (Eq. 3).

Re-oxidation of HS^- produced during sulfate reduction is also important in the Highborne mats. Aerobic chemolithotrophic oxidation of HS^- takes place at the O_2/HS^- interface, which is predominantly associated with the top of Layer 3 (Fig. 9). This aerobic process leads to a decrease in pH due to H^+ formation and results in $CaCO_3$ dissolution (Eq. 4a). In addition, anaerobic chemolithotrophic HS^- oxidation coupled to denitrification (Eq. 4b) may play a role in mat lithification. Although NO_3^- concentrations in Exuma Sound are low (~32 n*M*; Visscher and Bebout, unpublished results), low concentrations of NO_3^- do not necessarily indicate low microbial activity. In particular, NO_3^- additions to anoxic stromatolite slurries resulted in significant HS^- oxidation, indicating that there is a potential for denitrification. Moreover, certain species of sulfide-oxidizing bacteria may be capable of using either O_2 or NO_3^- for HS^- oxidation, as has been reported for several marine thiobacilli (e.g., Visscher and Taylor 1993). In contrast to aerobic HS^- oxidation, which

causes carbonate dissolution, anaerobic HS^- oxidation using NO_3^- induces $CaCO_3$ precipitation (Eq. 4b).

Clearly, the various processes involved in sulfur cycling in the Highborne mats lead to different $CaCO_3$ scenarios. Moreover, the relative importance of HS^- oxidation under different environmental conditions varies in time and space (Fig. 4), and production of intermediate sulfur compounds is expected (Visscher and Van Gemerden 1993, Van den Ende and Van Gemerden 1993). How these processes affect $CaCO_3$ precipitation and dissolution is currently under investigation.

Processes involved in sulfur cycling within the Exuma Cays mats are summarized in Figure 9. Due to the high biomass associated with Layer 3 and the location of the O_2/HS^- interface at the top of Layer 3, the most dynamic sulfur cycling occurs within this layer. Sulfate reduction enhances $CaCO_3$ precipitation throughout Layer 3 and is particularly active during the night. During the day, aerobic HS^--oxidation rates peak at the top of Layer 3, causing $CaCO_3$ dissolution. From late afternoon until after sunrise, HS^- oxidation under anaerobic (denitrifying) conditions may also be important, leading to $CaCO_3$ precipitation at the top of Layer 3. Such diel fluctuations in sulfur cycling would create alternating conditions of carbonate dissolution and precipitation at the oxic-anoxic interface. These processes could result in the truncation of previously microbored and weakened carbonate grains and reprecipitation of lithified micritic crusts at the top of Layer 3. Precipitation associated with sulfate reduction throughout Layer 3 would lead to net lithification of this layer. Carbonate dissolution at the top of Layer 3, associated with aerobic sulfide oxidation at the oxic-anoxic interface, provides an alternative to surface bioerosion (Macintyre et al. 1996) as a possible mechanism for truncation of grains at the tops of the lithified layers. The chemocline theory is attractive in that coupled processes of dissolution and reprecipitation of carbonate associated with diel fluctuations of aerobic and anaerobic sulfide oxidation at the chemocline could also account for the formation of micritic crusts above truncated grains.

Carbon consumption: Aerobic vs. anaerobic metabolism

The importance of sulfur cycling in the formation of lithified micritic laminae in Exuma stromatolites is also apparent when consumption of organic carbon via aerobic and anaerobic (sulfate-reducing) processes is examined. Rates of aerobic respiration in the stromatolitic mats are higher than rates of sulfate reduction. However, aerobic respiration depends directly on photosynthesis by cyanobacteria and is limited to the light period, whereas sulfate reduction continues throughout the diel cycle. Assuming 12 h of photosynthetic O_2 production and aerobic respiration restricted to the top 3–4 mm, aerobic respiration is estimated to consume approximately 750–950 nmol/cm^2/d $\{CH_2O\}$ (Eq. 2). Sulfate reduction takes place in the top 10 mm during the entire diel cycle, and the rate is lower during the oxic period than during the anoxic period (Fig. 7). Since the SO_4^{2-}:$\{CH_2O\}$ stoichiometry is 2 (Eq. 3), sulfate reduction accounts for a total carbon consumption of approximately 470 nmol/cm^{-2}/d $\{CH_2O\}$. As a result, sulfate reduction facilitates a substantial net $CaCO_3$ precipitation. Photosynthesis, coupled to aerobic respiration, has no net effect on $CaCO_3$ (Eqs. 1 and 2), whereas photosynthesis coupled to sulfate reduction gains 1.5 $CaCO_3$ per $\{CH_2O\}$ recycled (Eqs. 1 and 3). When taking re-oxidation of HS^- produced during sulfate reduction into consideration, photosynthesis coupled to sulfur cycling (i.e., sulfate reduction and sulfide oxidation) still gains $CaCO_3$ by a factor of 1 or 1.3 under oxic (Eqs. 1, 3, and 4a) and anoxic conditions (Eqs. 1, 3, and 4b), respectively.

Comparison with non-lithifying microbial mats

Modern microbial mats such as those found in Guerrero Negro, Mexico (Canfield and Des Marais 1991), Solar Lake, Sinai (Jørgensen and Cohen 1977; Krumbein et al. 1977), Sabkha Gavish, Sinai (Krumbein et al. 1979), and Texel, The Netherlands (Visscher and Van Gemerden 1993), are commonly viewed as modern analogs of ancient stromatolitic microbial communities (Ward et al. 1989; Des Marais 1990). However, an important difference between these mats and ancient stromatolites is that the former are unlithified, whereas ancient stromatolites formed as actively mineralizing structures. Although the mats at Solar Lake (Lyons et al. 1984), Sabkha Gavish (Krumbein et al. 1979; Gavish et al. 1985), and Guerro Negro (J. Farmer, personal communication) contain diffuse precipitates of $CaCO_3$, lithified micritic crusts, the characteristic features of ancient stromatolites, do not form in these mats. This raises the question why benthic microbial mats building ancient stromatolites and stromatolites in the Exuma Cays form lithified micritic laminae, whereas others do not. Although this is undoubtedly a complex question, our results suggest that one critical factor may be iron availability

In hypersaline and marine microbial mats, the FeS pool typically exceeds the HS^- pool by several orders of magnitude (Jørgensen and Cohen 1977; Visscher and Van Gemerden 1993). In these mats, HS^- reacts rapidly with available iron to form an insoluble precipitate of FeS according to the reaction: $HS^- + Fe(OH)_2 \rightarrow FeS + OH^- + H_2O$ (Canfield and Berner 1987). Hence, most of the HS^- produced during sulfate reduction is not available for immediate reoxidation, but is immobilized as FeS. The low availability of Fe^{2+} in other Bahamian sediments (Till 1970) suggests that [FeS] is also low in Exuma stromatolites. This low concentration of iron may account for a much more dynamic sulfur cycling than has been found in other microbial mats. Even though the population of sulfate-reducing bacteria is two to three orders of magnitude smaller and sulfate reduction rates are one-half to five times less than in non-lithifying mats (Fründ and Cohen 1992; Visscher et al. 1992; Jørgensen 1994), the absence of reactive Fe^{2+} allows for the immediate biological oxidation of HS^-. As a result of a rapid re-oxidation of HS^- in Exuma Cay stromatolites, the sulfate reduction

rates reported in this paper may have been underestimated. As a consequence, the importance of sulfur cycling and associated lithification, compared to the effects of aerobic respiration, may be even greater than suggested by the calculations above.

Other factors that may affect lithification include differences in the biomass of individual layers. Layers 1 and 3 of Exuma mats contain more biomass, and therefore biogeochemical gradients are more strongly developed in these layers than in Layer 2. In addition, strong hydrodynamic regimes and greater porosity of Highborne Cay stromatolites compared to unlithified mats from other localities may enable a more efficient and rapid transport of organic carbon (and inorganic nutrients) from Layers 1 and 2, where carbon is produced by photosynthesis, to Layer 3, where it is consumed by sulfate reduction.

Summary and conclusions

Lithified micritic horizons, which define lamination in stromatolite-forming microbial mats in the Exuma Cays, Bahamas, are correlated with layers of high biomass. Microbial processes (biomass activities) within these stratified mats (Fig. 9) produce distinctive patterns of lithification as follows:

(1) Photosynthesis and respiration are high in Layers 1 (high biomass) and 2 (low biomass), causing precipitation and dissolution of $CaCO_3$. The balance of these processes results in little or no net lithification in these layers, depending on the amount of organic carbon produced by photosynthesis that is used for aerobic (vs. anaerobic) respiration.

(2) Sulfate reduction is high in Layer 3 (high biomass), where it causes $CaCO_3$ precipitation. This results in a lithified layer in which carbonate sand grains are cemented together by micritic precipitates. The depth to the top of Layer 3 is controlled by the amount of photosynthetic production of $\{CH_2O\}$ by cyanobacteria in Layer 1 and the amount of consumption of $\{CH_2O\}$ by sulfate-reducing bacteria in Layer 3.

(3) Sulfide oxidation at the oxic-anoxic interface at the top of Layer 3 may have a twofold effect: coupled processes of dissolution and precipitation associated with aerobic and anaerobic HS^- oxidation may result in etching and truncation of previously microbored grains and the precipitation of hard, micritic crusts; these crusts resemble micritic laminae found in ancient stromatolites.

These findings indicate a close correlation between dynamic sulfur cycling and the formation of lithified micritic laminae in stromatolite-forming microbial mats in the Exuma Cays. We are currently continuing our investigations of sulfur cycling within these mats to determine the spatial and temporal separation of intermediate reactions involved in sulfide oxidation. Our ultimate goal is to understand the general role of sulfur cycling in the formation of lithified micritic laminae in stromatolites over geologic time.

Acknowledgments

This study was financially supported by NSF grants OCE 9619314 (to P.T.V.) and OCE 9530215 (to R.P.R.). We thank participants of the Research Initiative on Bahamian Stromatolites (RIBS) for active discussion; Mark Feldmann for help with mat dissection; Alan Decho for providing *Schizothrix* EPS; Kathleen Browne, Jack Farmer and David DesMarais for valuable comments on the manuscript; Gary Grenier and Bob Dzombia for technical assistance; and the crew of the R/V Calanus for logistic support. RIBS Contribution Number 1.

References cited

Awramik, S.M. (1992) The history and significance of stromatolites. In M. Schidlowski et al., Eds., Early Organic Evolution: Implications for Mineral and Energy Resources, p. 435–449. Springer-Verlag, Berlin.

Awramik, S.M. and R. Riding (1988) Role of algal eukaryotes in subtidal columnar stromatolite formation. Proceedings of the National Academy of Science, 85, 1327–1329.

Bertrand-Sarfati, J. (1976) An attempt to classify late Precambrian stromatolite microstructures. In M.R. Walter, Ed., Stromatolites. Developments in Sedimentology, 20, 251–259. Elsevier, New York.

Canfield, D.E. and Berner, R.A. (1987) Dissolution and pyritization of magnetite in anoxic marine sediments. Geochimica et Cosmochimica Acta, 51, 645–659.

Canfield, D.E. and Des Marais, D.J. (1991) Aerobic sulfate reduction in microbial mats. Science, 251, 1471–1473.

Chafetz, H.S. and Buczynski, C. (1992) Bacterially induced lithification of microbial mats. Palaios, 7, 277–293.

Dalrymple, D.W. (1965) Calcium carbonate deposition associated with blue–green algal mats, Baffin Bay, Texas. Institute of Marine Science Publication, 10, 71–85.

De Man, J. (1975) The probability of most probable numbers. European Journal of Applied Microbiology 1, 67–78.

Des Marais, D.J. (1990) Microbial mats and the early evolution of life. Trends in Ecology and Evolution 5, 140–145.

Dill, R.F., Shinn, E.A., Jones, A.T., Kelly, K., and Steinen, R.P. (1986) Giant subtidal stromatolites forming in normal salinity water. Nature, 324, 55–58.

Dravis, J.J. (1983) Hardened subtidal stromatolites, Bahamas. Science, 219, 385–386.

Feldmann, M. (1995) Controls on stromatolite formation: a comparative study of modern stromatolites from the Bahamas with Messian examples from southeast Spain. Ph.D. thesis, Swiss Federal Institute of Technology, Zurich, 128 p.

Fossing, H. and Jørgensen, B.B. (1989) Measurement of bacterial sulfate reduction in sediments: evaluation of a single-step chromium reduction method. Biogeochemistry, 8, 205–222.

Friedman, G.M., Amiel, A.J., Braun, M., and Miller, D.S. (1973) Generation of carbonate particles and laminites in algal mats—example from sea-marginal hypersaline pool, Gulf of Aqaba, Red Sea. Journal of Sediment Petrology, 52, 41–46.

Fründ, C. and Cohen, Y. (1992) Diurnal cycles of sulfate reduction under oxic conditions in microbial mats. Applied and Environmental Microbiology, 58, 70–77.

Gavish, E., Krumbein, W.E., and Halvey, J. (1985) Geomorphology, mineralogy and groundwater geochemistry as factors of the hydrodynamic system of the Gavish Sabkha. In G.M. Friedman and W.E. Krumbein, Eds., Ecoligical Studies, Hypersaline Ecosystems, vol. 53, p. 186–217. Springer Verlag, Berlin.

Gerdes, G., Krumbein, W.E., and Holtkamp, E. (1985) Salinity and water activity related zonation of microbial communities and potential stromatolites of the Gavish Sabkha. In G.M. Friedman and W.E. Krumbein, Eds., Ecoligical Studies, Hypersaline Ecosystems, vol. 53, p. 238–266. Springer Verlag, Berlin.

Golubic, S. and Browne, K.M. (1996) *Schitzothrix gebeleinii* sp. nova builds subtidal stromatolites, Lee Stocking Island, Bahamas. Algological Studies, 83, 273–290.

Hines, M.E., Visscher, P.T., and Devereux, R. (1996) Sulfur Cycling. In S.Y. Newell et al., Eds., Manual of Environmental Microbiology:

Aquatic Environments, p. 324–334. American Society for Microbiology, Washington, D.C.

Jørgensen, B.B. (1990) A thiosulfate shunt in the sulfur cycle of marine sediments. Science, 249, 152–154.

———(1994) Sulfate reduction and thiosulfate transformation in a cyanobacterial mat during a diel oxygen cycle. FEMS Microbiology Ecology, 13, 303–312.

Jørgensen, B.B. and Cohen, Y. (1977) Solar Lake (Sinai). 5. The sulfur cycle of the benthic cyanobacterial mats. Limnology and Oceanography, 22, 657–666.

Krumbein, W.E. (1979) Photolithotrophic and chemoorganotrophic activity of bacteria and algae as related to beachrock formation and degradation (Gulf of Aqaba, Sinai). Geomicrobiology Journal, 1, 139–203.

Krumbein, W.E., Cohen, Y., and Shilo, M. (1977) Solar Lake (Sinai). 4. Stromatolitic cyanobacterial mats. Limnology and Oceanography, 22, 635–656.

Krumbein, W.E., Buchholz, H., Franke, P., Giani, D., Giele, C., and Wonneberger, K. (1979) O_2 and H_2S coexistence in stromatolites. Naturwissenschaften, 66, 381–389.

Lyons, W.B., Long, D.T., Hines, M.E., Gaudette, H.E., and Armstrong, P.B. (1984) Calcification of cyanobacterial mats in Solar Lake, Sinai. Geology, 12, 623–626.

Macintyre, I.G., Reid, R.P., and Steneck, R.S. (1996) Growth history of stromatolites in a fringing Holocene reef, Stocking Island, Bahamas. Journal of Sedimentary Research, 66, 231–242.

Monty, C.L.V. and Mas, J.R. (1981) Lower Cretaceous (Wealdian) blue-green algal deposits of the province of Valencia, eastern Spain. In C. Monty, Ed., Phanerozoic Stromatolites, Case Histories, p. 85–120. Springer-Verlag, New York.

Reid, R.P. and Browne, K.M. (1991) Intertidal stromatolites in a fringing Holocene reef complex in the Bahamas. Geology, 19, 15–18.

Reid, R.P., Macintyre, I.G., Steineck, R.S., Browne, K.M., and Miller, T.E. (1995) Stromatolites in the Exuma Cays: Uncommonly common. Facies, 33, 1–18.

Revsbech, N.P. and Jørgensen, B.B. (1985) Microelectrodes: their use in microbial ecology. Advances in Microbial Ecology, 9, 293–352.

Riding, R. (1994) Stromatolite survival and change: the significance of Shark Bay and Lee Stocking Island subtidal columns. In W.E. Krumbein, D.M. Paterson, and L.J. Stal, Eds., Biostabilization of Sediments, p. 183–202. Oldenburg, Germany.

Riding, R., Awramik, S.M., Winsborough, B.M., Griffin, K.M., and Dill, R.F. (1991) Bahamian giant stromatolites: microbial composition of surface mats. Geological Magazine, 128, 227–234.

Steneck, R.S., I.G. Macintyre, and R.P. Reid. (1997) Unique algal ridge systems of Exuma Cays, Bahamas. Coral Reefs, 16, 29–37.

Till, R. (1970) The relationship between environment and sediment composition (geochemistry and petrology) in the Bimini Lagoon. Journal of Sedimentary Petrology, 40, 367–385.

Van den Ende, F.P. and van Gemerden, H. (1993) Sulfide oxidation under oxygen limitation by a *Thiobacillus thioparus* isolated from a marine microbial mat. FEMS Microbiology Ecology, 13, 69–78.

Vasconcelos, G., McKenzie, J.A., Bernasconi, S., Grujic, D., and Tien, A.J. (1995) Microbial mediation as a possible mechanism for natural dolomite formation at low temperature. Nature (London), 337, 220–222.

Vasconcelos, G. and McKenzie, J.A. (1997) Microbial mediation of modern dolomite precipitation and diagenesis under anoxic conditions (Lagoa Vermelha, Rio de Janeiro, Brazil). Journal of Sedimentary Research, 67, 378–390.

Visscher, P.T. and van Gemerden, H. (1991) Production and consumption of dimethylsulfoniopropionate in marine microbial mats. Applied and Environmental Microbiology, 57, 3237–3242.

———(1993) Sulfur cycling in laminated marine ecosystems. In R.S. Oremland, Ed., Biogeochemsitry of Global Change: Radiatively Active Trace Gases, p. 672–693. Chapman and Hall, New York.

Visscher, P.T. and Taylor, B.F. (1993) A new mechanism for anaerobic metabolism of dimethyl sulfide. Applied and Environmental Microbiology 59, 3784–3789.

Visscher, P.T. and van den Ende, F.P. (1994) Diel and spatial fluctuations of sulfur transformations. In L.J. Stal and P. Caumette, Eds., Microbial Mats, Development and Environmental Significance, p. 353–360. Springer Verlag, Berlin.

Visscher, P.T., Beukema, J., and van Gemerden, H. (1991) In situ characterization of sediments: measurements of oxygen and sulfide profiles. Limnology and Oceanography, 36, 1476–1480.

Visscher, P.T., Prins, R.A., and van Gemerden, H. (1992) Rates of sulfate reduction and thiosulfate consumption in a marine microbial mat. FEMS Microbiology Ecology, 86, 383–294.

Walter, M.R. (1983) Archaen stromatolites: evidence of the Earth's earliest benthos. In J.W. Schopf, Ed., Earth's Earliest Biosphere, its origin and evolution, p. 187–213. Princeton University Press, Princeton, New Jersey.

Walter, L.M., Bischof, S.A., Patterson, W.P., and Lyons, T.W. (1993) Dissolution and recrystallization in modern shelf carbonates: evidence from pore water and solid phase chemistry. Philosophical Transactions of Royal Society London A, 344, 27–36.

Ward, D.M., Weller, R., Shiea, J., Castenholz, R.W., and Cohen, Y. (1989) Hot spring microbial mats: anoxygenic and oxygenic mats of possible evolutionary significance. In Y. Cohen and E. Rosenberg, Eds., Microbial Mats: Physiological Ecology of Benthic Microbial Communities American Society for Microbiology, p. 3–15. Washington, D.C.

Manuscript received March 9, 1998
Manuscript accepted August 6, 1998
Paper handled by Jillian F. Banfield